Intermolecular Adhesion in Conjugated Polymers

Jeremy D. Schmit
Department of Physics, Brandeis University Waltham, MA 02454

Alex J. Levine
Department of Chemistry & Biochemistry and The California Nanosystems Institute UCLA, Los Angeles, CA 90095-1596

(Dated: February 5, 2008)

Conjugated polymers are observed to aggregate in solution. To account for this observation we propose a inter-chain binding mechanism based on the intermolecular tunneling of the delocalized π-electrons occurring at points where the polymers cross. This tunneling mechanism predicts specific bound structures of chain that depend on whether they are semiconducting or metallic. Semiconducting chains should form polyacene-like states exhibiting binding at every other site, while (doped) metallic chains can bind at each site. We also show that solitons co-localize with the intermolecular binding sites thereby strengthening the binding effect and investigate the conformational statistics of the resulting bimolecular aggregates.

PACS numbers: 82.35.Cd,83.80.Rd,61.25.Hg

Conjugated polymers are of great fundamental interest in that they are exotic, low-dimensional (semi-) conductors[1, 2]. More recently the use of such polymers has been explored in a variety of applications ranging from optical [3, 4] and electronic[5] devices to biosensors[6]. While exploring their use as highly sensitive biosensors, researchers[7] discovered their surprising tendency to aggregate into multi-molecular filaments. This aggregation is even more surprising in that it occurs in a system of strongly charged conjugated polymers dissolved in low ionic strength aqueous solutions.

Motivated by this observation, we investigate more generally a potential aggregation mechanism that should play a role in any π-conjugated system. In this letter we propose that the appearance of intermolecular electronic states made possible by π-electron wavefunction overlap where two conjugated polymers cross leads to a large enough reduction of the electronic energy of the two polymer system to cause intermolecular binding even in dilute solution. The electronic intermolecular interaction draws localized states out of the continuum of extended states on each chain in a manner analogous to the formation of traditional bonding/anti-bonding orbitals. We examine the effect of this bonding mechanism in both semiconducting (SC) and doped metallic (M) polymers. In the case of the SC polymers we also examine the interaction of solitonic excitations on the chains with the binding sites. Finally we use the results of these analyses to predict the aggregated fraction of chains in solution and the change in the polymer conformational statistics that may be measured via scattering.

We find that the inter-chain electronic tunneling leads to a significant change in the electronic states far from the Fermi level. In SC polymers, this change makes energetically favorable a polyaclene-like conformation (see Fig. 2) with binding at every other site. In addition, there is a strong interaction between these inter-chain binding sites and solitonic excitations on the chain. Uncharged solitons are strongly attracted to the interchain binding points and, at room temperature, co-localize there further strengthening the inter-chain attractive interaction. Charged solitons, on the other hand, interact weakly with the tunneling sites at inter-chain crossing points. In M chains, however, the inter-chain electronic interaction favors the formation of a parallel polymer configuration where there is electronic tunneling at every site (see Fig. 2) and there are no solitonic excitation on the chains.

In either case the presence of intermolecular bonds changes the statistical properties of the conformations of the bound pairs primarily by modifying their effective persistence length. As the binding strength increases, the dominant deformation mode of the polymers goes from bond rotations in the free chains to localized bending at defects in the intermolecular bonding pattern for weakly bound chains, and finally to the elastic bending of stiff polymer bundles.

To consider the most simple description of conjugated polymers, we study a tight-binding model of noninteracting electrons based on the SSH Hamiltonian[1] for each polymer chain. At a specific set of sites α (*i.e.* the crossing points between chains) we allow inter-chain tunneling with the overlap integral $t' \simeq 0.2$eV [8]. Thus, we write for the single particle Hamiltonian

$$\begin{aligned} H &= \sum_{\ell,n} \left[-t_{\ell,\ell+1} (|\ell, n\rangle\langle \ell+1, n| + |\ell+1, n\rangle\langle \ell, n|) \right] \\ &- t' \sum_{\{\alpha\}} \left[|\alpha, 1\rangle\langle \alpha, 2| + |\alpha, 2\rangle\langle \alpha, 1| \right]. \end{aligned} \quad (1)$$

Here the $|\ell, n\rangle$ represents an electron on the ℓ^{th} tight-binding site of the n^{th} chain where the sum $\ell = 1, \ldots N$ extends over all sites and N is the polymerization index and $n = 1, 2$ labels the two chains. In the case of the undoped, homogeneously dimerized chain $t_{\ell,\ell+1} = t_0 + (-1)^\ell \frac{\Delta}{2}$. We expect $t \simeq 2.5$eV and $\Delta \simeq 0.5$eV[1].

For homogeneous the M chains (*i.e.* without the Peierls distortion) $\Delta = 0$.

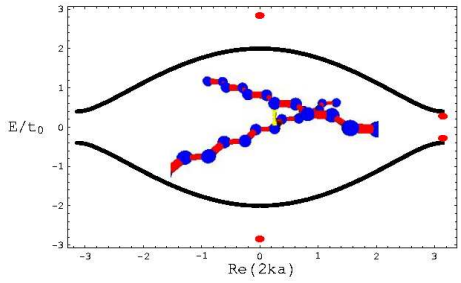

FIG. 1: (color online) The spectrum of electron states resulting from electronic intermolecular tunneling at the crossing point. The bound states are represented by the (red) filled circles at $\mathrm{Re}(k) = 0, \pi$. The schematic figure in the center represents such a single tunneling site between two crossing polymers.

We first consider a single crossing point between two homogeneous, infinite, undoped chains using a transfer matrix approach[9]. The Hamiltonian of the system commutes with the chain interchange operator so that the energy eigenstates have definite parity with respect to chain interchange. We find four bound states, two in each of the symmetric and antisymmetric sectors of the state space, at energies

$$E_b = \pm\sqrt{t_1^2 + t_2^2 + \frac{t'^2}{2} \pm \sqrt{4t_1^2 t_2^2 + t'^2(t_1^2 + t_2^2) + \frac{t'^4}{4}}}, \tag{2}$$

where we have defined: $t_{1,2} = t_0 \pm \frac{\Delta}{2}$. These bound states are represented as red circles on the band structure diagram shown in Fig. 1. There are two ultraband [10] states above and below the valance and conduction bands. These states are split from the band edges by $\mathcal{O}(t'^2/t_0)$ and their wavefunction decays over $\mathcal{O}(t_0/t')$ sites from the tunneling site. Due to this localization of the bound state wavefunction, two tunneling sites separated by more than this distance interact weakly. In addition, there are two states that appear symmetrically shifted by $\mathcal{O}(t'^2\Delta/t_0^2)$ into the gap. They have a real part of their wave number at the edge of the zone and localization length $\mathcal{O}(at_0^2/t'\Delta)$. The effect of the polymer ends on all of these localized states is insignificant unless the tunneling site is within a localization distance of the chain ends. For high molecular weight chains, we may ignore end effects.

The dominant part of the reduction of the system's electronic energy is due to the occupation of the lower ultraband state; the contribution of the gap state can be neglected. Similarly, the shifts in the extended states of the chains are small for high molecular weight chains since these shifts vanish as $O(N^{-1})$. Previous calculations on the M chains [11] demonstrate that the ultraband state is displaced by $2t[\sqrt{1 + t'^2/(4t^2)} - 1]$ below the bottom edge of the band, while, once again, the effect

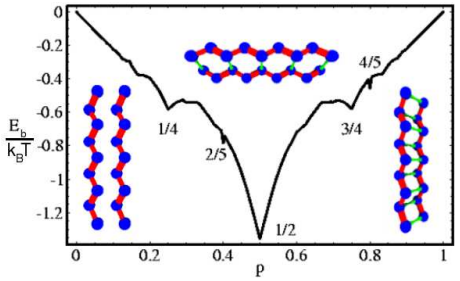

FIG. 2: (color online) The energy of the bound undoped chains as a function of the fraction p of (equally spaced) binding sites for $t' = 0.25$eV. The insets show (left to right) two free chains ($p = 0$), and the expected forms of the maximally bound SC chains at $p = 1/2$ and M (doped) chains at $p = 1$. The former structure is similar to polyacene except the binding results from the hybridization of the π_z orbitals.

of the shift in the continuum states and the gap state are irrelevant. In the case of both the M and SC chains, we note that the appearance of a single localized state centered at the crossing point of two polymers reduces the electronic energy of the chains by ~ 100meV.

We now consider the most energetically favorable configuration of the two chains in both the M and SC cases. Here we demonstrate a distinct difference between these two cases. Previous work on the M polymers has shown that the strongest interchain binding in the absence of chain electrostatic repulsion occurs for the parallel chain configuration as shown on the right side of Fig. 2. In this case the individual localized ultraband states below the band edge hybridize into a new filled band. As this result seems intuitively reasonable, it is surprising to find that in the case of the SC chains the parallel configuration of the two chains results in *no binding energy* at all.

One can understand this absence of intermolecular binding in the parallel configuration as follows. In this configuration the inter-chain interaction symmetrically splits the filled valance band of the SC polymer. Since the band remains well-separated from the similarly split conduction band there is no net energy reduction upon splitting. For the case of strong enough inter-chain tunneling ($t' \simeq \Delta$) so that the valance and conduction bands do not remain well separated, the Peierls distortion of the chains breaks down and returns the system to the case of M polymers[8]. Instead we find that the energy minima for SC chains is the polyacene-like structure shown in the middle cartoon in Fig. 2.

To explore this further we compute the electronic contribution to the binding energy by direct diagonalization of the two-chain Hamiltonian with 200 tight binding sites on each; the results are shown in Fig. 2. This figure is symmetric about the $p = 1/2$ tunneling site density that is the minimum energy configuration. The symmetry between binding site densities p and $1 - p$ can be understood as follows. Removing a single binding site from the fully linked chains can be represented by adding an inter-chain tunneling term to Eq. 1 with $t' \to -t'$. Thus

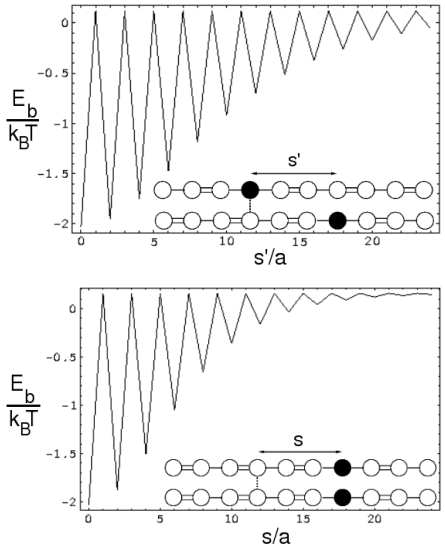

FIG. 3: The upper figure shows the interaction energy of two solitons one on each chain separated by s' lattice sites. One soliton is centered at the binding site. The lower figure shows the interaction energy of a pair of symmetrically placed solitons displaced from the binding site by s.

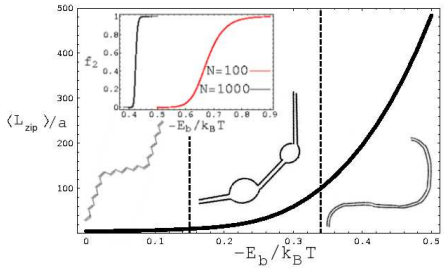

FIG. 4: (color online) The mean length $\langle L_{\rm zip}\rangle$ of the bound regions versus the binding E_b energy between tunneling sites on the two chains. The inset shows the fraction f_2 of bound chains as a function of E_b in dilute solution.

a single non-tunneling defect in the fully linked chains generates the same set of localized states as does an isolated tunneling site on the unlinked chain. From Eq. 2 both localized states lower the electronic free energy of the system by the same amount. We extend this argument to multiple non-tunneling defects in the otherwise fully linked chains by noting that the associated localized states simply hybridize to a degree that depends on their spatial separation. At any finite density of regularly spaced tunneling (non-tunneling) defects the localized states form a narrow "impurity" band, but the symmetry between the two cases is unchanged. The effect of quenched spatially randomness in the distribution of the tunneling (non-tunneling) sites on the energy of the system is minimal [11].

In SC chains the inter-chain binding interaction is complicated by disorder in the dimerization pattern that takes the form of solitons. These defects may arise due to either end effects, *cis-* insertions in the *trans-* chain, or light electron/hole doping[1, 12]. We now explore the interaction between these solitons and the binding sites on the two chains by considering two chains linked at one tunneling site and examining the energy spectrum of the system as function of the relative positions of the solitons from the binding site.

First, we posit that each chain contains a single soliton and vary the position of a the inter-chain tunneling site with respect to the positions of the soliton. See the inset of Fig. 3b for schematic diagram. In moving the tunneling site, we require the tunneling site to remain on equivalent sites on the two chains to preserve the simultaneous diagonalization of the Hamiltonian and the chain interconversion operator. Initially, we approximate the soliton as a single-site shift in the dimerization. We consider a more physical model of a spatially extended soliton below, but this simplified model captures the basic effect of the solitons in an analytically tractable manner.

The single site soliton introduces new localized states at energies E given by the roots of the polynomial,

$$0 = E^3 - E(4[t_0^2 + \Delta^2] + t'^2) \pm 8t'\Delta, \qquad (3)$$

where the upper (lower) sign applies to the chain anti-symmetrized (symmetrized) states. For large E we find bound states at $E \simeq (4[t_0^2{+}\Delta^2]{+}t'^2)^{1/2}$ similar to the previously discussed ultraband states. For small E, however, we find a pair of gap states with energy $E \simeq \pm t'\Delta/t_0$ that are symmetrically positioned about the mid-gap of the SC chain. These are remnants of the usual soliton associated mid-gap states of the two chains split by the tunneling matrix element t'. The mid-gap state associated with an uncharged soliton on the chain is singly occupied so that the splitting of these states allows for the double occupancy of the lower state resulting in a reduction of the system's energy upon the creation of the inter-chain tunneling site. The localization of an uncharged soliton on each chain at their crossing point further lowers their electronic energy by $\Delta/t' \simeq 2.5$ enhancing the binding energy at that site. In contrast, for the case of charged solitons (as would occur on lightly doped, SC polymers) both mid-gap states on each chain are filled there is no further energy reduction due to the co-localization of the charged solitons with the binding site.

To extend this result to more physical solitons we put one SSH soliton of width $7a$ at the center of each chain and numerically calculate the binding energy for the $N = 199$ chains. The interaction energy between the SSH solitons and the tunneling site is shown in Fig. 3. We find that the solitons are attracted to the inter-chain tunneling site. The width of this potential well for solitons is broadened once one soliton reaches the binding site. The interaction potential between the solitons and the binding site is oscillatory because the soliton associated mid-gap states have nodes on alternating sites.

The formation of these bimolecular assemblies will ef-

fect the photophysics of the system[13] as well as the conformational statistics of the polymers in solution. As the site binding energy E_b is increased there is an abrupt condensation of the polymers in dilute solution into bimolecular filaments. See the inset of Fig. 4. We do not consider aggregation into larger supramolecular assemblies. The persistence length of the bimolecular filaments has three distinct regimes as a function of E_b. In the limit of a vanishing E_b, conformations of the free chains may be approximated as a freely jointed chain with a Kuhn length of $l_{\min} \sim 10a$[14] where a is the length of a unit cell. For $E_b \gg k_{\rm B}T$ the bimolecular filaments saturate their available binding sites, and the intermolecular bonds hinder bond rotations so that the softest deformation mode involves bending in the conjugation plane. Using known bond bending and stretching constants[1, 15], we estimate that the persistence length is $\ell_{\max} \sim 100a$. Between these extremes, where defects in the intermolecular binding are typically separated by less than $\ell_{\max}$, the chain tangents decorrelate primarily due to the essentially free rotations at those defects. Thus the bimolecular filaments will have a continuously varying persistence length $\ell_{\rm P}$, $\ell_{\min} < \ell_{\rm P} < \ell_{\max}$ and their effective persistence length is determined by the mean length of the fully bound chain segments $\langle L_{\rm zip}\rangle$.

We solve for this mean length $\langle L_{\rm zip}\rangle$ using a modified Poland-Scheraga (PS) model[16]. The partition function for the partially bound pair of chains each containing N sites may be written as

$$Z(N) = \sum_{p} \sum_{\{i_\pi^{(1)}, i_\pi^{(2)}, j_\pi\}} \prod_{\pi=0}^{p} u(i_\pi^{(1)}, i_\pi^{(2)}) v(j_\pi), \qquad (4)$$

where $u(i_\pi^{(1)}, i_\pi^{(2)})$ is the Boltzmann weight of the $\pi^{\rm th}$ unbound region consisting of $i_\pi^{(1)} + i_\pi^{(2)}$ tight binding sites where the superscript indexes the two chains. $v(j_\pi)$ is the corresponding Boltzmann weight associated with a bound region of j_π consecutive sites. The sum in Eq. 4 is constrained by the fixed total number of tight binding sites. We relax this constraint using the Grand Canonical ensemble and, from the PS technique we compute the free energy $F = -k_B T N \ln(x_1)$ where x_1 is the root of

$$\frac{x(x-v)}{xv - v^2(1-\sigma)} = \sum_{n=1}^{\infty} e^{-\pi \ell_{min}/n} \left(\frac{u}{x}\right)^n \left(\frac{n}{2}\right)^{-c}. \qquad (5)$$

Here $v = \exp(-E_b/k_{\rm B}T)$ is the Boltzmann weight of a single binding site, while $u \simeq \exp(a/\ell_p) \approx 1$ is the exponentiated entropy of a segment of unbound chain. The exponent $c \simeq 2.1$ reflects the loss of entropy in these unbound regions due to self avoidance and the loop closure condition [17]. Finally, $-k_B T \ln \sigma$ is the domain wall energy between bound and unbound regions accounting for local chain bending energy. The fraction of binding sites is given by $\theta = \partial \ln x_1 / \partial \ln v$ and the mean length of bound regions $\langle L_{\rm zip}\rangle$ may be computed from the ratio of θ, to the fraction of sites at the boundary of bound and unbound regions, θ_b. The results are shown in Fig. 4. For $E_b < 0.4 k_{\rm B}T$, $\langle L_{\rm zip}\rangle < \ell_{\max}$. Thus, given the best estimate of t' and for $N > 10^3$, chains will aggregate in dilute solution (10^{-5}M) into this intermediate state where the persistence length is continuously controlled by E_b. Measurements of the persistence length may test the estimates of t' arising from quantum chemical calculations, however, there are other contributions to E_b including the electrostatic repulsion between *e.g.* the highly charged, water soluble polymers. More direct tests of this theory necessitate measurements on more chemically simple π-conjugated systems such as polyacetylene.

Understanding the persistence length of bimolecular filaments may play a role in controlling the penetration of such polymers into microporous or zeolitic structures. Future work will explore conjugated gels formed at higher polymer concentrations.

JS was supported by the MRSEC Program of the National Science Foundation under Award No DMR00-80034. The authors would like to thank Fyl Pincus for valuable discussions.

[1] W.P. Su, J.R. Schrieffer, and A.J. Heeger, Phys. Rev. Lett., **42**, 1698 (1979); W.P. Su, J.R. Schrieffer, and A.J. Heeger, Phys. Rev. B, **22**, 2099 (1980).
[2] H. Takayama, Y.R. Lin-Liu, and K. Maki, Phys. Rev. B, **21**, 2388 (1980).
[3] B.J. Schwartz Annu. Rev. Phys. Chem. **54**, 141 (2003).
[4] R.H. Friend, *et al.*, Nature **397**, 121 (1999).
[5] F. Garnier *et al.* Science **265**, 1684 (1994).
[6] L.H. Chen *et al.* Proc. Natl. Acad. Sci. (USA), **96**, 12287 (1999).
[7] D.L. Wang, J. Lal, D. Moses, G.C. Bazan, and A.J. Heeger, Chem. Phys. Lett., **348**, 411 (2001).
[8] J.L. Brédas, J.P. Calbert, D.A. da Silva Filho, and J. Cornil, Proc. Natl. Acad. Sci. **99**, 5804 (2002).
[9] J.D. Schmit and A.J. Levine in progress.
[10] S.R. Phillpot, D. Baeriswyl, A.R. Bishop, and P.S. Lomdahl, Phys. Rev. B, **35**, 7533 (1987).
[11] J.D. Schmit and A.J. Levine, Phys. Rev. E **71**, 051802 (2005).
[12] S. Roth and H. Bleier Adv. Phys. **36**, 385 (1987).
[13] C. Daniel *et al.* J. Chem. Phys. **123**, 084902 (2005).
[14] C. L. Gettinger, A. J. Heeger, J. M. Drake and D. J. Pine, J. Chem. Phys. **101**, 1673 (1994).
[15] M. Canales and G. Sesé, J. Chem. Phys. **118**, 4237 (2003).
[16] D. Poland and H. A. Scheraga, *Theory of Helix-Coil Transistions in Biopolymers*, Academic Press, New York (1970).
[17] Y. Kafri, D. Mukamel, L. Peliti, Phys. Rev. Lett. **85**, 4988 (2000).